Stability of Eukaryotic Flagellar Beating to Noise and Mechanical Perturbations

Kirsty Y. Wan and Raymond E. Goldstein
Department of Applied Mathematics and Theoretical Physics, Centre for Mathematical Sciences, University of Cambridge, Wilberforce Road, Cambridge CB3 0WA, United Kingdom
(Dated: June 12, 2014)

The eukaryotic flagellum is a remarkable cellular structure, for it can sustain beating with unfailing rhythmicity, yet is capable of rapid responses to stimuli. Recent studies have revealed flagellar beating to be intrinsically noisy, but detailed understanding of this stochasticity is lacking. Here, we use *Chlamydomonas reinhardtii* to investigate flagellum sensitivity to noise and perturbations. We find that flagellum oscillations prescribe stable limit cycles and phase-dependent waveform fluctuations, while interbeat intervals exhibit approximate $1/f$ noise and long-range correlations spanning hundreds of beats. By forcing beating flagella with hydrodynamic loads, we quantify the recovery of periodic breastroke beating from imposed perturbations. These results will help constrain microscopic theories on the origin and regulation of beating.

Patterns of coordinated movement in living organisms, such as walking, running, and galloping, may be variable yet simultaneously stable. Such repetitive dynamics are distinguished by their reproducibility, sustainability over long times, and stability in the presence of small to moderate perturbations. In the precise, rhythmic beating of the flagella of the alga *Chlamydomonas* we find remarkable living oscillators that fulfil these three criteria. The synchronous beating of its twin flagella allows *Chlamydomonas* to swim a fast breaststroke [1]. For this alga, oscillations of its flagella are *self-sustained* – repeated mechano-chemical cycles continuously supply energy to motor dyneins residing within flagellar axonemes [2]. Stepping action of individual motors is intrinsically stochastic [3], and yet, beating can nevertheless persist, resilient against a cacophony of biochemical and background fluctuations [4]. Often, in assessing the fidelity or robustness of a biological oscillator, the stability and rhythmicity of its oscillations serve as prime indicators: one might identify pathological gaits of human walking from measures of cycle stability [5], determine the phase-dependent response of circadian clocks using external stimuli [6], or infer the health of a human heart from variability of inter-beat intervals [7, 8]. Similarly, periodic oscillations of beating flagella are correlated with a cell's responses and sensitivity to its environment, but study of these features remains inchoate [9–14].

Here, we assess flagellum stability on two complementary levels, drawing on data from a large population ($\sim$100) of cells. First, we evaluate stability to weak fluctuations originating from such sources over which the experimenter has little control. These include background thermal noise, intracellular biochemical processes associated with cell metabolism [15], or even fluctuations in photon irradiance [4]. Flagellar dynamics are found to be inherently stable, but waveform noise displays an intriguing phase dependence. Measured beat-to-beat intervals form a complex timeseries that exhibits fractal structure, and successive beats may remain correlated for many seconds. Second, we measure the recovery of flagellar beating in the aftermath of stronger, externally-derived perturbations imposed by injecting fluid impulses near a beating flagellum. Post-perturbation, the normal breaststroke resumes following a characteristic relaxation dynamics back to the stable limit cycle. This ability to recover readily from disruption to beating may be a crucial property of viable ciliary/flagellar structures.

To permit long-time, in-focus visualization of flagellar dynamics, wildtype cells (strains CC124 and CC125, *Chlamydomonas* Center) were individually caught and held in place by micropipette micromanipulation (Patchstar, Scientifica, UK) with gentle suction, as described previously [9, 12]. High-speed images (SA3 Fastcam, Photron, USA and Phantom V311, Vision Research, USA) of beating flagella were captured at $1000-3000$ frames/s – at least one order of magnitude above the maximum flagella beat frequency. Continuous recordings ($1-10$ minutes) were taken for each cell, from which $\sim 1-5\times10^3$ contiguous beat cycles could be extracted. Recordings were conducted under conditions that appropriately mimic a wild-type cell's natural daytime habitat, namely white light illumination (100W halogen lamp) with negligible background lighting, and hence some phototactic response is expected [16]. Pixel coordinates that

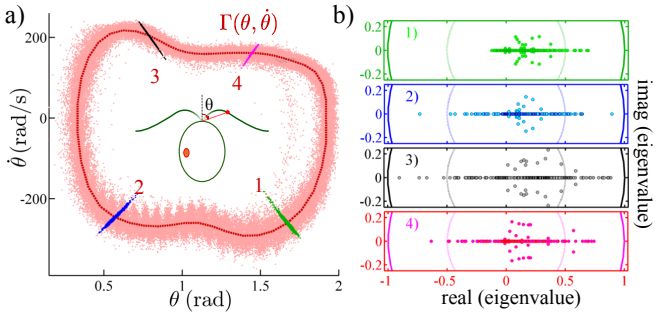

FIG. 1. (color online) Noisy flagellar limit cycles. a) Trajectories in angle (θ) – angular velocity ($\dot\theta$) space at a fixed arclength along the flagellum, with four Poincaré sections shown. b) Lyapunov exponents at phases 1-4, for 48 cells.

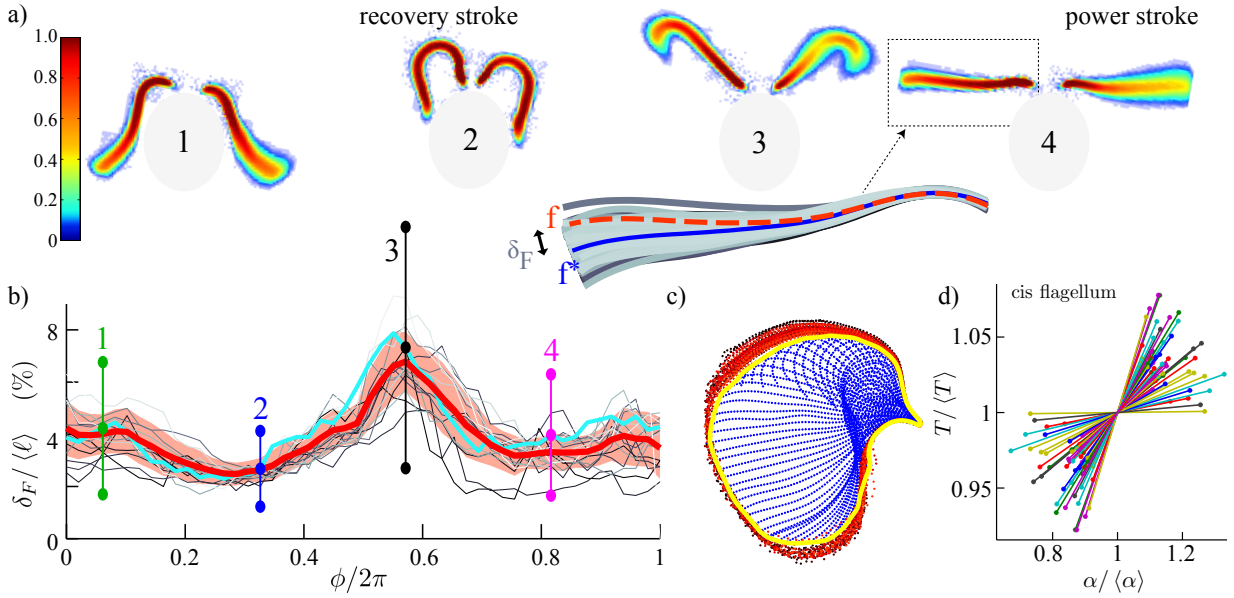

FIG. 2. (color online) Noisy flagellar waveforms. a) Overlaid waveforms at phases 1–4 (Fig. 1a), colored by recurrence. Observed stroboscopically, flagellar waveforms $\mathbf{f}$ coalesce in a band about an average shape $\mathbf{f}^*$. b) Length-normalized Fréchet distance $\delta_F(\mathbf{f},\mathbf{f}^*)/\ell$, where ℓ is the total flagellum length, showing phase-dependent noise. (Cyan: average over $\mathcal{O}(10^3)$ beat cycles for a single cell; error bars: one s.d. from the mean. Red: a multicell average; shading: one s.d. from mean.) c) Discretized points (blue) along a flagellum define an area *per beat* via an alpha-shape (yellow). This shape fluctuates over successive beat cycles (red). d) Positive correlation between per-beat area α and per-beat period T, for multiple cells. Lines drawn summarize the per-cell noisy scatter, chosen to be coincident with the major axes of 95% confidence ellipses, sampling a χ^2 distribution.

track the flagellum in each frame were converted to spline fits, and used to generate timeseries.

Automated flagellar waveform tracking has given us access to unprecedented spatio-temporal resolution [12], and recording *Chlamydomonas* flagellar beating over thousands of cycles allows us to measure the degree of spatial reproducibility. Angles $\theta(t)$ traced by a point at fixed arclength along the waveform relative to a reference axis (Fig. 1a) serve as convenient projections of the multidimensional dynamics. From θ and $\dot{\theta}$ we create a cloud of points mapping the attracting region around a limit cycle Γ, which we approximate numerically. Progression through each cycle is charted by associating the $2D$ flagellum centerline $\mathbf{f}(t_i)$ at each time t_i with a uniformly-rotating phase ϕ defined by transforming the polar angle [12]. Trajectory crossings $C = \{\mathbf{x}_n : \phi(\mathcal{P}^n(\mathbf{x}_n)) = \phi_0,\ n = 1,2,3,\ldots\}$ at fixed $\phi = \phi_0$ correspond to iterations of a Poincaré return map $\mathcal{P}$.

To determine cycle stability, we computed for each cell, and for 50 subdivisions of $[0, 2\pi]$, eigenvalues of the Jacobian matrix of derivatives $\mathcal{J} = D\mathcal{P}|_{\mathbf{p}^*}$ taking $\mathbf{p}^* = \langle\mathbf{x}\rangle_{\mathbf{x}\in C}$, and fitting to the bilinear model $(\mathbf{x}_{n+1} - \mathbf{p}^*) = \mathcal{J}(\mathbf{x}_n - \mathbf{p}^*)$. The distribution of computed eigenvalues is shown in Fig. 1b, which is particularly dense on the real line. All eigenvalues have magnitude less than unity; limit cycles are stable. Further, we ascertain whether these stable flagellar oscillations exhibit phase-dependent noise, by taking into account the full dimensionality of flagellar waveforms. Define $S_k = \{\mathbf{f}(t_j^k)\}$ to be the set of equal-phase waveforms where $\{j : \phi(t)|_{t=t_j^k} = \phi_k\}$, for phases $\phi_k = 2\pi k/50$, $k = 1, \cdots 50$; this selection criteria is equivalent to observing stroboscopically periodic waveforms (Fig. 2a). We measure the dissimilarity between curves $\mathbf{f} \in S_k$ and an average waveform $\mathbf{f}_k^*$ by the *Fréchet distance* $\delta_F(\mathbf{f}, \mathbf{f}_k^*)$ between curves, where for $\mathbf{x}, \mathbf{y} : [\mathbf{0}, \mathbf{1}] \to \mathbf{R^2}$ some arbitary $2D$ curves and parameterizations γ_x and γ_y,

$$\delta_F(\mathbf{x},\mathbf{y}) = \inf_{\gamma_x,\gamma_y} \max_{u\in[0,1]} \{|\mathbf{x}(\gamma_x(u)) - \mathbf{y}(\gamma_y(u))|\} \ . \quad (1)$$

Computationally, the minimizing operation makes use of the Fréchet distance matrix $F_\epsilon = \{t \in [0,1] \times [0,1] : |\mathbf{x} - \mathbf{y}| \le \epsilon\}$, with flagellar waveforms approximated by polygonal curves [17]. At each phase, δ_F gauges waveform noise in the periodic formation of the flagellum shape (Fig. 2b), which we find is minimized during the recovery stroke ($\gtrsim 1.7\%$) and maximized at the transitions between power and recovery strokes ($\lesssim 10.8\%$).

What governs transitions between strokes? The classic eukaryotic flagellum has a distinctive '9+2' structure [2] of microtubule doublets, and periodic flagellar beating emerges from selective activation and inactivation of dyneins that crosslink them. To determine when and where this putative switch-point between power and recovery strokes occurs, we measured the beat frequency and waveform envelope of each full beat cycle. The nth beat cycle was systematically defined by partition-

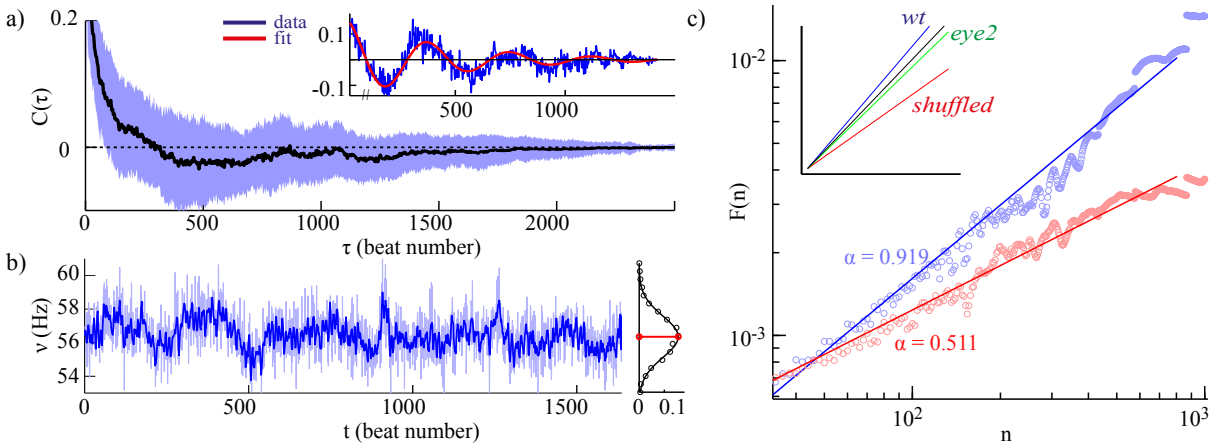

FIG. 3. (color online) Long-range correlations in flagellar beating. a) Autocorrelation in interbeat intervals $b(t)$ for a population of cells: average (black), and one s.d. from the mean (shaded region). Inset: parametric fit to $C(\tau)$ for a sample cell. b) Fluctuations in $\nu(t) := 1/b(t)$ for a sample cell, with the filtered signal overlaid on the raw data to highlight global trends, and pdf fit to a Gaussian. c) DFA on a sample $b(t)$ timeseries and its shuffled version. Inset: DFA scaling for a blind mutant (*eye2*) lies between that of the *wt* and *wt*-shuffled. (Linear fits have been displaced vertically for better visualization.)

ing flagellar positions by phase. Averaged measurements from two different Poincaré sections were taken for the instantaneous per-cycle beat period T_n, and frequency $\nu_n = 1/T_n$. To approximate the nth-cycle beat envelope we construct the *alpha-shape* [18], defined here by the set K of material points along the flagellum (Fig. 2c) and a collection $\{S_r\}$ of closed discs of radii r. That is, for $S_r^c = Cl(\mathbf{R}^2 \backslash S_r)$ the closure complement of S_r and $D = \bigcup \{S_\alpha^c : S_r^c \supset K\}$ we compute a straight-line graph approximation to its piecewise-circular boundary ∂D, starting from the (closest-point) Delaunay triangulation of K (Matlab, Mathworks). We chose $r = 5$ pixels ~ 1.11 μm, and denote the computed alpha-shape area by α_n (Fig. 2c), where n indexes beat number. We find T_n and α_n to be correlated (Fig. 2d). A similar correlation has been found independently [14]. Plotting $\Pi = T_n / \langle T_n \rangle$ vs $A = \alpha_n / \langle \alpha_n \rangle$ reveals directional but noisy scatter. To determine this directionality we compute the matrix

$$\mathrm{Cov}\,[\Pi, A] = \begin{pmatrix} \langle \mathcal{T}\mathcal{T} \rangle & \langle \mathcal{T}\mathcal{A} \rangle \\ \langle \mathcal{A}\mathcal{T} \rangle & \langle \mathcal{A}\mathcal{A} \rangle \end{pmatrix} , \qquad (2)$$

where $\mathcal{T} = \Pi - \langle \Pi \rangle$ and $\mathcal{A} = A - \langle A \rangle$. For cell i we estimate $\gamma_i = \Pi / A \sim \tan^{-1}(v_2/v_1)$ where (v_1, v_2) is the principal eigenvector direction. For the ensemble we find $\langle \gamma_i \rangle \sim (0.264 \pm 0.146)$ rad. We derive a dimensional ratio of increments $\delta A / \delta \Pi = \left\langle \left\langle \alpha_n^i \right\rangle / \left\langle T_n^i \right\rangle \times (1/\tan(\gamma_i)) \right\rangle_{\text{all } i} \approx 39.7 \pm 31.0$ μm^2/ms. Equivalently, assuming a flagellum "wingspan" of 10μm during the power stroke this is $\delta \ell / \delta \Pi \sim 4\mu$m/ms, for an effective amplitude ℓ. The observed correlation may be rationalized thus: if η is the medium viscosity and $\nu \sim T^{-1}$ is the angular frequency of the beat, a rod-like flagellum of length ℓ produces a motive force $F(\ell, T) \sim \eta \ell^2 / T$. Then here $F(\ell + \delta\ell, T + \delta T) - F(\ell, T) \approx (a\delta\ell - b\delta T)$, $a \approx b$, consistent with constant force production by motors along the axoneme. A similar argument holds for the power density $p = P/\ell$ where the power $P \sim \eta T^{-2} \ell^3$.

In the presence of small perturbations due to weak environmental fluctuations, both flagellum and cell may be feedback modulating their behavior in real-time. With sufficient resolution, we can measure not only the magnitude of such responses but also their temporal correlation. It is instructive to consider $b(t)$, the timeseries of beating periods, and the statistic $C(\tau) = \langle b(t+\tau)b(t) - \langle b \rangle^2 \rangle$, where $\langle \cdot \rangle$ denotes a time average. The decay of $C(\tau)$ is unexpectedly slow, and in many cases even oscillatory (Fig. 3a), which suggests an underlying periodic process with noise. Consider $b(t) = b_0(1+\beta(t))\cos(\omega_0 t + \phi(t))$, where b_0 and ω_0 are the averaged amplitude and frequency of these oscillations, and $\beta(t)$, $\phi(t)$ are independent functions respectively characterizing phase and amplitude noise. We assume that $\beta(t)$ is stationary, and that $\phi(t)$ is a Brownian motion with $\langle \phi(t) \rangle = 0$ and $\langle \phi(t)^2 \rangle = Dt$. The autocorrelation is

$$\tilde{C}(\tau) = \frac{b_0^2}{2}[1 + C_b(\tau)]\mathrm{e}^{-D|\tau|}\cos(\omega_0 \tau) , \qquad (3)$$

where C_b is the covariance of $\beta(t)$. For a sample cell, we fit $C(\tau)$ using (3) above, with an empirical function $C_b(\tau) = \beta e^{-|\tau|/\xi}$ (Fig. 3a), yielding $b_0 = 0.157$, $D = 0.002$, $\omega_0 = 0.016$, $\beta = 9.928$ and $\xi = 1.85$. In particular we find a timescale for the periodicity of slow oscillations: $2\pi/\omega_0 = 392$ beats, or 6.01 s. Sampled over 65 cells, the average form of $C(\tau)$ takes $\sim$250 beats for the correlation to reverse sign, and persists over $\sim$1000 beats, or $\sim$15 s.

Next, we perform a detrended fluctuation analysis (DFA) on $b(t)$ to obtain a scalar measure of 'noisiness' of timeseries with fractal structure [19]. For a signal $b(t)$ of length L we construct the mean-subtracted, integrated series $B(t) = \sum_{i=0}^{L} (b(t_i) - \langle b \rangle)$, divide B into

K non-overlapping sections of size $n = L/K$, $\{I_i := [t_i, t_{i+1}], t_i = iL/K, i = 1, 2, \cdots, K-1\}$, and compute the local trend at the ith section. Let $B_n(t_i)$ be the lsq linear fit to data points $B(t_i \in I_i)$. We detrend B by subtracting B_n, and compute

$$F(n) = \left(\frac{1}{K} \sum_{i=1}^{K} (B(t_i) - B_n(t_i))^2 \right)^{0.5} . \qquad (4)$$

A power-law scaling $F(n) \sim n^\alpha$ can be seen to hold (Fig. 3c). For the population, we obtain $\alpha = 0.83 \pm 0.10$ (67 cells, $\mathcal{O}(10^3)$ successive beats for each). Randomly permuting $b(t)$ (each time averaging over 10 shuffles) yields $\alpha = 0.48 \pm 0.03$, or white noise. DFA on a blind *Chlamydomonas* mutant with *wildtype* motility (*eye2*, CC4302 Chlamydomonas Center) gives $\alpha = 0.72 \pm 0.04$ (Fig. 3d), consistent with reduced flagellum noise upon removal of photo-perception. Wildtype *Chlamydomonas* respond to single-photon events [4], that alter voltage-gated flagellar Ca^{2+} channels downstream [20] and elicit characteristic flagellar responses in $\mathcal{O}$(ms). For our light source we estimate an incident flux of 5×10^{17} photons s^{-1} m^{-2} on an illuminated sample, which falls on a maximum of 3×10^4 rhodopsins in the eyespot of a single cell [21], each spanning ~ 1 $\mathring{A}^2$ in area [22]. A held cell may therefore only encounter up to 100 photons over the course of a single beat, yet the timescale we measure for slow oscillations (Fig. 3a) is orders of magnitude greater than that of response to photon fluctuations.

Intracellular calcium is the putative biochemical source for control of flagellar beating [23, 24], and is directly implicated in our measured slow oscillations in beat frequency. In previous work [9] we found that the flagella of freeswimming *Chlamydomonas* cells switch stochastically from synchronous to asynchronous beating (drifts) with a characteristic timescale of ~ 10 s, and suggested that this could be a consequence of fluctuating levels of internal calcium, which is known to affect the *cis* and *trans* flagella differentially. Here we find oscillatory beat frequency correlations in synchronous breaststroke beating, and conjecture that dynamic changes in coupled flagellar behavior leading to synchronous/asynchronous transitions corresponds to stochastic crossings of a calcium threshold. Fluctuations of $\mathcal{O}(s)$ have been observed in *in vivo* measurements of cytosolic calcium in *Chlamydomonas* cells ballistically-loaded with calcium dyes [25].

In their native habitats cilia and flagella experience disturbances imparted through the fluid: flagella of microalgae must respond to encountered physical obstacles, likewise mammalian cilia must withstand changes in viscoelastic loading [26]. To mimic such perturbations, pulses of fluid were manually introduced from a 2nd pipette placed in the vicinity of a beating flagellum, applying forces of $\mathcal{O}(nN)$. Such an affected flagellum undergoes a number of abnormal beats before resumption of normal beating. Greater out-of-plane deformations appear when greater perturbative forces are applied. For small perturbations beating remains confined to the plane, enabling dynamic flagellar tracking (Fig. 4a). As in the unperturbed case (Fig. 1), we can now compute perturbed trajectories $r(t)$ and phases. To estimate the attractor strength, we define

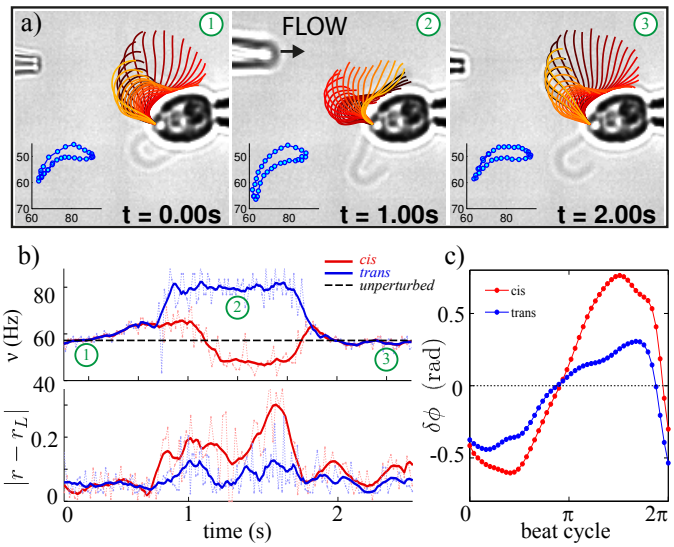

FIG. 4. (color online) Stability to perturbations. (a) Fluid injected from a 2nd pipette (arrow) alters beating of *both* flagella (1-3). Here waveforms for the *cis* flagellum only are overlaid. Insets: x-y coordinates of a reference point at fixed arclength. (b) Deviation from pre-perturbation limit cycle and instantaneous frequency during one perturbation event. (c) The response in the flagellum is phase-dependent.

$$\sigma = \frac{1}{t} \ln \left| \frac{\mathbf{r}(0) - \mathbf{r}_L(0)}{\mathbf{r}(t) - \mathbf{r}_L(t)} \right| , \qquad (5)$$

for $\mathbf{r}(t)$ assumed to contract linearly towards the pre-perturbation limit cycle $\mathbf{r}_L(t)$. Interestingly perturbing one flagellum can lead to altered beating of both flagella in a coupled pair (Fig. 4b), confirming their shared biochemical origins. For 57 perturbed-flagella events, we find $\sigma \sim 2.94 \pm 1.72$ s^{-1} or $\sigma^{-1} \sim 20.4$ beats, for a beat frequency of 60 Hz. Perturbed oscillations are also phase-shifted by $\delta\phi = \phi_{\text{new}} - \phi_{\text{old}}$ (Fig. 4c). Reversing the forcing direction (sucking fluid back through pipette) produces a qualitatively different response, highlighting the directional sensitivity of flagellar beating.

These external forces/flows are detected by membrane pressure sensors [27], which in conjunction with homeostatic inputs from the cytosol and eyespot, lead to rapid feedback responses that are difficult to quantify or monitor molecularly. Here, we have chosen to address global, generic properties of rhythmic flagellum behaviors, using dynamic high-resolution flagellar tracking to conclude that flagellar beating is (i) noisy but intrinsically stable, (ii) exhibits long-range correlations, and that (iii)

flagellum noise is phase-dependent. We attribute flagellum noise primarily to fluctuations in calcium. The long-timescale beat frequency correlations we measure may be signatures of spatial and temporal calcium signalling [28]; calcium is already known to govern ciliary beat frequencies in many different organisms [29–31]. Oscillatory calcium dynamics would vastly improve flagellum signalling specificity, as signals can be integrated over longer times without detrimental, sustained rise. It would be interesting to examine the noise spectrum of artificial flagellar beating, where feedback-regulation would be absent.

We thank M. Polin, K.C. Leptos, and P. Holmes for discussions. Financial support is acknowledged from the EPSRC, ERC Advanced Investigator Grant 247333, and a Senior Investigator Award from the Wellcome Trust.

[1] T. J. Racey, R. Hallett, and B. Nickel, Biophys. J. **35**, 557 (1981).
[2] K. A. Wemmer and W. F. Marshall, Curr. Biol. **14**, R992 (2004).
[3] C. Shingyoji, H. Higuchi, M. Yoshimura, E. Katayama, and T. Yanagida, Nature **393**, 711 (1998).
[4] P. Hegemann and W. Marwan, Photochem. Photobiol. **48**, 99 (1988).
[5] S. M. Bruijn, O. G. Meijer, P. J. Beek, and J. H. van Dieen, J. R. Soc. Interface **10**, 20120999 (2013).
[6] I. Mihalcescu, W. H. Hsing, and S. Leibler, Nature **430**, 81 (2004).
[7] Y. Ashkenazy, P. C. Ivanov, S. Havlin, C. K. Peng, A. L. Goldberger, and H. E. Stanley, Phys. Rev. Lett. **86**, 1900 (2001).
[8] P. C. Ivanov, M. G. Rosenblum, C. K. Peng, J. Mietus, S. Havlin, H. E. Stanley, and A. L. Goldberger, Nature **383**, 323 (1996).
[9] M. Polin, I. Tuval, K. Drescher, J. P. Gollub, and R. E. Goldstein, Science **325**, 487 (2009).
[10] R. E. Goldstein, M. Polin, and I. Tuval, Phys. Rev. Lett. **103**, 168103 (2009).
[11] K. C. Leptos, K. Y. Wan, M. Polin, I. Tuval, A. Pesci, and R. E. Goldstein, Phys. Rev. Lett. **111**, 158101 (2013).
[12] K. Y. Wan, K. C. Leptos, and R. E. Goldstein, Journal of the Royal Society Interface **11**, 20131160 (2014).
[13] V. F. Geyer, F. Juelicher, J. Howard, and B. M. Friedrich, Proceedings of the National Academy of Sciences of the United States of America **110**, 18058 (2013).
[14] R. Mai, G. S. Klindt, I. H. Riedel-Kruse, F. Julicher, and B. M. Friedrich, arXiv:1401.7036 [q-bio.CB] (2014).
[15] H. Sakakibara, H. Kojima, Y. Sakai, E. Katayama, and K. Oiwa, Nature **400**, 586 (1999).
[16] U. Ruffer and W. Nultsch, Cell Motil. Cytoskeleton **41**, 297 (1998).
[17] T. Eiter and H. Mannila, Technical Report CD-TR 94/64, Information systems Department, Technical University of Vienna, Austria (1994).
[18] H. Edelsbrunner, D. G. Kirkpatrick, and R. Seidel, Ieee Transactions On Information Theory **29**, 551 (1983).
[19] C.-K. Peng, S. V. Buldyrev, S. Havlin, M. Simons, H. E. Stanley, and A. L. Goldberger, Phys. Rev. E **49**, 1685 (1994).
[20] R. Uhl and P. Hegemann, Biophysical Journal **58**, 1295 (1990).
[21] K. W. Foster and R. D. Smyth, Microbiol. Rev. **44**, 572 (1980).
[22] O. A. Sineschchekov, Light In Biology and Medicine, Vol 2 , 523 (1991).
[23] M. Bessen, R. B. Fay, and G. B. Witman, J. Cell Biol. **86**, 446 (1980).
[24] C. G. DiPetrillo and E. F. Smith, J. Cell Biol. **189**, 601 (2010).
[25] G. L. Wheeler, I. Joint, and C. Brownlee, Plant Journal **53**, 401 (2008).
[26] N. T. Johnson, M. Villalon, F. H. Royce, R. Hard, and P. Verdugo, American Review of Respiratory Disease **144**, 1091 (1991).
[27] K. Fujiu, Y. Nakayama, A. Yanagisawa, M. Sokabe, and K. Yoshimura, Curr. Biol. **19**, 133 (2009).
[28] S. Luan, ed., *Coding and decoding of calcium signals in plants* (Springer, 2011).
[29] J. H. Evans and M. J. Sanderson, Cell Calcium **26**, 103 (1999).
[30] T. Hayashi, M. Kawakami, S. Sasaki, T. Katsumata, H. Mori, H. Yoshida, and T. Nakahari, Exp. Physiol. **90**, 535 (2005).
[31] M. Salathe and R. J. Bookman, Journal of Physiology-london **520**, 851 (1999).